Characterization of acoustic metasurface absorbers usingnumerical methods including viscous and thermal losses

Andersen, Peter Risby; Cutanda Henriquez, Vicente; Godinho, Luis; Chazot, Jean-Daniel; Carbajo San Martín, Jesús

Published in:
Proceedings of internoise 2019

Publication date:
2019

Document Version
Publisher's PDF, also known as Version of record

MADRID
inter.noise 2019
June 16 - 19
NOISE CONTROL FOR A BETTER ENVIRONMENT

Characterization of acoustic metasurface absorbers using numerical methods including viscous and thermal losses

Risby Andersen, Peter[1]
Centre for Acoustic-Mechanical Micro Systems, Technical University of Denmark
Ørsteds Plads, Building 352, DK-2800, Kgs. Lyngby, Denmark

Cutanda Henríquez, Vicente [2]
Centre for Acoustic-Mechanical Micro Systems, Technical University of Denmark
Ørsteds Plads, Building 352, DK-2800, Kgs. Lyngby, Denmark

Godinho, Luis[3]
ISISE, Dept. Civil Engineering, University of Coimbra
Rua Luis Reis Santos, Coimbra, 3030-788 Coimbra, Portugal

Chazot, Jean-Daniel [4]
Sorbonne Universités, Université de Technologie de Compiègne, laboratoire Roberval
FRE CNRS, Centre de recherche Royallieu, CS 60319, 60203 Compiègne cedex

Carbajo San Martín, Jesús [5]
Dept. Physics, Systems Engineering and Signal Theory, University of Alicante
Carretera San Vicente del Raspeig s/n, 03690, Alicante, Spain

ABSTRACT

Acoustic meta-surfaces are periodic structures commonly realised using sub-wavelength sized resonators. One of their possible applications is in noise control where they can be applied to create very compact sound absorbers. Numerical modelling and characterization of meta-surfaces require the inclusion of acoustic viscous and thermal dissipation effects. Several variations of numerical methods are available that include such losses, each having different computational benefits and limitations. In this work, numerical methods that incorporate dissipation are applied to study the normal absorbing properties of several meta-surface designs.

[1]prand@elektro.dtu.dk
[2]vcuhe@elektro.dtu.dk
[3]lgodinho@dec.uc.pt
[4]jean-daniel.chazot@utc.fr
[5]jesus.carbajo@ua.es

The results will be used to both benchmark the different numerical methods, but also to extract data for simplified fluid equivalent models that can be used as input for large-scale simulations including meta-surfaces.

Keywords: Numerical methods, viscothermal losses, sound absorption, meta-surfaces
I-INCE Classification of Subject Number: 34

INTRODUCTION

In recent years, acoustic meta-surfaces have gained attention due to their potential to absorb low-frequency sound waves while having an effective size much smaller than the wavelength [1]. Meta-surfaces are usually realized using periodically organized acoustic sub-wavelength resonators, such as Helmholtz resonators [2, 3] or more exotic shaped resonators [4].

Modeling of meta-surface requires the inclusion of viscothermal effects. Existing theory for acoustic wave propagation in uniform tubes of arbitrary cross-section shape [5] can be used to characterize simple acoustic meta-surface absorbers by means of a fluid equivalent model. In this approach, the viscous and thermal losses of the meta-surface are taken into account by means of its complex dynamic density and bulk modulus on a macroscopic scale [6]. These models can thus be easily incorporated in large-scale numerical simulations by describing the meta-surface as an equivalent fluid in terms of these effective properties. Unfortunately, the fluid equivalent approach presents some limitations, especially for the analysis of more complex geometries. In fact, in many cases it is desirable to improve the compactness of a meta-surface by introducing more design freedom, thus making the use of this approach inadequate. In such cases, numerical methods that include losses are necessary to accurately characterize and optimize the performance of meta-surfaces. Both the Finite Element Method (FEM) and the Boundary Element Method (BEM) can incorporate such losses, each having their strengths and drawbacks.

Some authors have proposed models based on the FEM [7–11] and the BEM [12–14] which rely on the Full-Linearized Navier Stokes (FLNS) formulation to capture both viscous and thermal dissipation effects in narrow geometries. Until recently, these implementations were unfeasible due to the high computational cost associated with high-density meshes necessary to appropriately resolve the viscous and thermal boundary layers. Nevertheless, the high development of computers over the past decades has paved the way for the use of such implementations in more acoustic problems each passing day. Some examples of the use of FLNS-based models for the acoustic characterization of metamaterials can be found in [15, 16]. In these works, the importance of accounting for the visco-thermal dissipation effects when analysing the acoustic wave propagation through double-negative acoustic metamaterials is shown. As opposed to the fluid equivalent approach, these numerical models are generic and can handle any arbitrary geometry. In most cases, it may not only result in a much more accurate approach to characterize complex meta-surface absorbers but also serve to explain the acoustic behaviour thereof. On the other hand, numerical models could also be used to cross-check the adequacy of using a fluid equivalent model to study a specific structure.

In this work, three test cases based on unconventional shaped Helmholtz resonators are studied, and their frequency dependent absorbing capabilities are obtained by numerical methods. The test cases chosen represent configurations that might be difficult to model with analytical methods. The focus will mainly be on two BEM implementations, namely

a full method relying on the Kirchhoff decomposition (KD-BEM) and an approximate method using the boundary layer impedance (BLI-BEM) method. Additionally, FLNS-FEM simulations will be included for comparison. The test cases will mainly serve as benchmarks to study the different numerical implementations with acoustic viscothermal losses.

NUMERICAL METHODS WITH LOSSES

In this section and subsections, we will present the theory behind three different numerical methods that are used to include the effect of viscous and thermal losses into acoustic simulations.

FEM based on the full linearized Navier-Stokes formulation

Acoustic viscous and thermal dissipation can be included in the FEM by discretization of the time-harmonic Full Linearized Navier-Stokes (FLNS) equations, that is, the conservation of mass, energy and momentum equations, given by

$$i\omega\rho + \rho_0 \nabla \cdot \vec{v} = 0, \tag{1}$$

$$i\omega\rho_0 C_p T - \lambda \Delta T - i\omega p = 0 \tag{2}$$

$$i\omega\rho_0 \vec{v} = -\nabla p + \left(\mu_B + \frac{4}{3}\mu\right) \nabla(\nabla \cdot \vec{v}) - \mu \nabla \times \nabla \times \vec{v}, \tag{3}$$

respectively. In Equations 1-3, the acoustic variables are the pressure p, the temperature T, the velocity $\vec{v}$ and the density ρ. Additionally, the fluid properties are expressed from ρ_0, C_p, λ, μ_B and μ which are the static density, the specific heat at constant pressure, the thermal conductivity, the bulk viscosity, and the shear viscosity, respectively. Finally, the frequency of oscillation is determined by the angular frequency ω. Several strategies exist to discretize the FLNS [7–11]. Perhaps, the most common approach is to eliminate the density variations by substitution of the ideal gas law into Equation 1 leaving three equations having pressure, temperature, and velocity as the unknown variables [11, 17]. Simulations in the following rely on the implementation of the FLNS found in the commercial software COMSOL Multiphysics. It is reasonable to assume that the heat capacity of the boundary Γ in most cases is much larger than air, as a result, the temperature fluctuations at the boundary can be considered as an isothermal process, so

$$T \approx 0 \quad \text{on} \quad \Gamma. \tag{4}$$

Additionally, the air molecules closest to a boundary will tend to stick to the boundary resulting in a no-slip condition of the velocity, with

$$\vec{v} = \vec{v}_b \quad \text{on} \quad \Gamma, \tag{5}$$

where $\vec{v}_b$ is the boundary velocity. As a consequence of the boundary conditions in Equations 4-5, so-called thermal and viscous boundary layers will form, creating a transition region close to the boundary where the acoustic temperature and velocity

fluctuations change rapidly. In general, if air is considered the medium of propagation, the thickness of the thermal and viscous boundary layers are of similar size, ranging from millimeters to micro-meters in the audible frequency range. When performing FEM simulations based on the FLNS it is necessary to create special boundary layer meshes that can capture the acoustic behavior in the boundary layer region.

BEM based on the Kirchhoff decomposition

Applying the BEM directly to the FLNS equations is not straightforward. Hence, it is convenient to manipulate the FLNS into a form more suitable for the BEM. Therefore, previous boundary element implementations rely on the so-called Kirchhoff decomposition, where the fundamental equations are split into an acoustic, thermal and viscous mode given by p_a, p_h and $\vec{v}_v$, respectively. Each of the modes is described independently by the Helmholtz equations [18]

$$\Delta p_a + k_a^2 p_a = 0, \tag{6}$$

$$\Delta p_h + k_h^2 p_h = 0, \tag{7}$$

$$\Delta \vec{v}_v + k_v^2 \vec{v}_v = \vec{0} \quad \text{with} \quad \nabla \cdot \vec{v}_v = 0 \tag{8}$$

in the domain, and only couples at the boundary through the coupling conditions

$$T = \tau_a p_a + \tau_h p_h \approx 0 \quad \text{on} \quad \Gamma, \tag{9}$$

$$\vec{v}_b = \phi_a \nabla p_a + \phi_h p_h + \vec{v}_v \quad \text{on} \quad \Gamma, \tag{10}$$

where k_a, k_h, and k_v are the acoustic, thermal and viscous wavenumbers, respectively, and τ_a, τ_h, ϕ_a and ϕ_h are complex and frequency dependent coupling constants. While Equation 6 behaves similarly to the isentropic Helmholtz equation, the thermal pressure and viscous velocity in Equations 7-8 are rapidly decaying in the vicinity of boundaries and act more like diffusion equations. Equations 6-8 are discretized using collocation BEM with continuous quadratic elements and coupled following the approach found in Ref. [13] and adapted to two-dimensions in Ref. [19]. Previous implementations of the BEM are directly based on the work by Bruneau et al. [18]. In their work, the acoustic and thermal wavenumbers are developed using a second-order Taylor expansion. However, the expansion is, in general, unnecessary and the full expression can be used without any additional computational cost. It should be noted, that comparative studies between the Taylor expanded and full wavenumbers has shown no significant differences. However, for completeness we will in this work use the full expressions of the wavenumbers, expressed as

$$k_a^2 = \frac{2\left(\frac{\omega}{c}\right)^2}{X + R} \qquad \text{and} \qquad k_h^2 = \frac{2\left(\frac{\omega}{c}\right)^2}{X - R}, \tag{11}$$

with

$$X = 1 + (l_v + \gamma) l_h \frac{1}{c}(i\omega), \tag{12}$$

$$R = \left(1 + 2\left[l_v - (2 - \gamma) l_h\right] \frac{1}{c}(i\omega) + (l_v - \gamma l_h)^2 \frac{1}{c^2}(i\omega)^2\right)^{1/2} \tag{13}$$

where γ is the ratio of specific heats, c is the speed of sound in air, l_v is the viscous characteristic length and l_h is the thermal characteristic length. The two characteristic lengths are defined by

$$l_v = \frac{\frac{4}{3}\mu + \mu_B}{\rho_0 c} \qquad \text{and} \qquad l_h = \frac{\lambda}{\rho_0 c C_p}. \tag{14}$$

One of the benefits of the KD-BEM (Kirchhoff Decomposition-BEM) is that boundary layer meshing is avoided. On the other hand, the system is solved using several Shur complement styled operations and the acoustic BEM matrices arising from Equation 6 are dense.

BEM based on the boundary layer impedance method

A simpler alternative to the KD-BEM is the implementation of the BEM together with a Boundary Layer Impedance (BLI). Indeed, for this implementation only the classic Helmholtz equation needs to be solved, accounting for the linear acoustic behaviour of the system. The governing equation can thus be written as

$$\Delta p + k_0^2 p = 0 \tag{15}$$

where k_0 is the isentropic wavenumber. The effect of possible thermal and viscous losses occurring along the boundaries of the discretized propagation domain is accounted for by imposing a special boundary condition. Although several possibilities can be found in the literature, such as in the work by Bossart et al. [20] or Schmidt and Thöns-Zueva [21], the authors here use the Wentzel-type boundary condition suggested by Nijhof [22] and Berggren et al. [23], with the form

$$-\delta_v \frac{i-1}{2} \Delta_T p + \delta_T k_0^2 \frac{(i-1)(\gamma-1)}{2} p + \frac{\partial p}{\partial n} = 0 \tag{16}$$

In Equation 16, n is the boundary normal component and Δ_T represents the sum of the second order spatial derivatives in the tangent directions, δ_v, and δ_T are, respectively, the viscous and thermal acoustic boundary-layer thicknesses, which can be defined as

$$\delta_v = \sqrt{\frac{2\nu}{\omega}} \qquad \text{and} \qquad \delta_t = \sqrt{\frac{2\lambda}{\omega \rho_0 C_p}}. \tag{17}$$

ν being the kinematic viscosity of air. To obtain the results presented throughout this paper, the BEM was implemented using quadratic discontinuous elements (i.e. with 3 internal nodes per element), which allows a simple evaluation of second-order spatial derivatives required in Equation 16. While the method offers a computational complexity similar to the isentropic wave equation, care must be taken when the geometric dimensions are small and the boundary layers might overlap [23].

TEST CASES

In the following, three study cases are tested. In each case, we want to observe the effect of viscothermal dissipations on the normal incident sound absorption coefficient. Narrow sections are therefore introduced for different configurations. The walls are considered as rigid, and an acoustic excitation is imposed with an incident plane wave on one side. The pressure field is then calculated with the previous models.

Test case 1

The first test case is the oblique narrow section presented in Figure 1. In 2D the narrow section represents a slit. The pressure field could be described with a fluid model and equivalent properties given by Stinson [5] or Johnson-Champoux-Allard [6] approach . The interest here is, therefore, to compare the FLNS and BEM models on a simple well-known geometry, and eventually with a simpler equivalent fluid model.

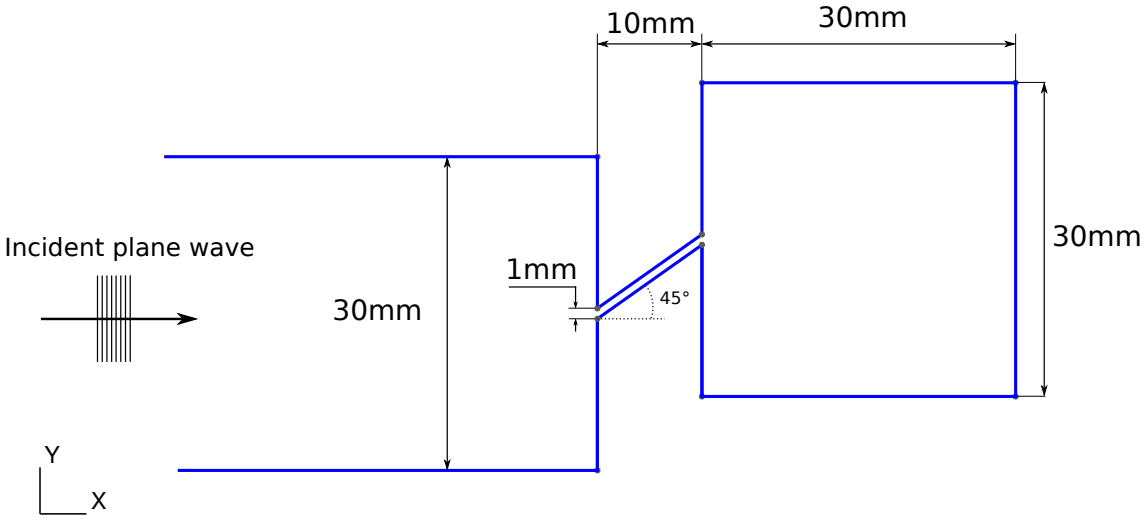

Figure 1: Test case 1

Test case 2

The second test case is a narrow section with an intermediate expansion chamber as presented in Figure 2. The expansion chamber has a uniform section and could be described as a dead-end pore in a fluid equivalent model, even though some modeling difficulties would arose in the intersections. The interest here is to see the convergence of the BEM models compared to the FLNS model with that additional geometrical complexity.

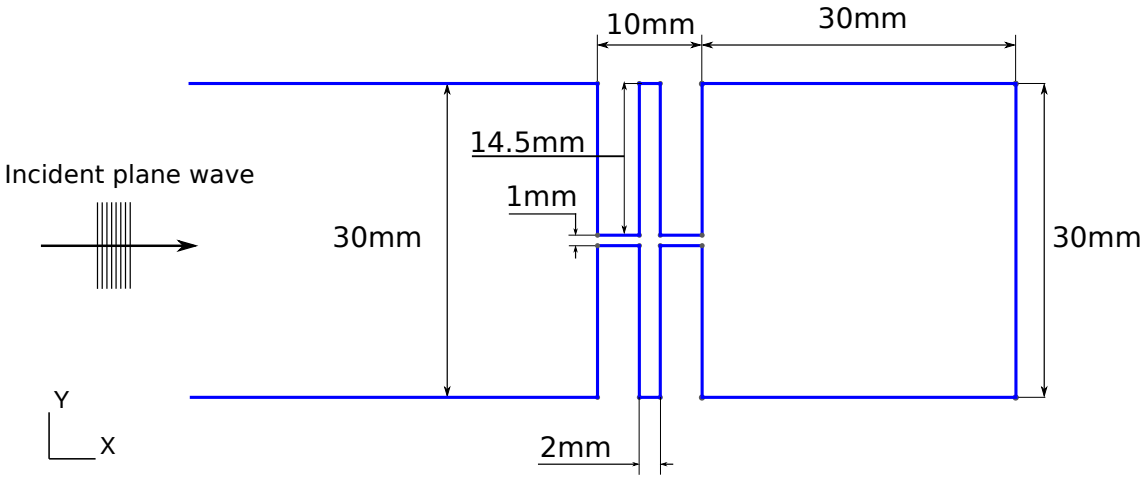

Figure 2: Test case 2

Test case 3

The third test case is a narrow section with an intermediate expansion chamber as presented in Figure 3. Contrary to the previous case, the section of the expansion chamber is not uniform but varies linearly. In this case, though possible, it is more difficult to describe the pressure field with an equivalent fluid. It is however very interesting to compare the FLNS and the BEM results in this non-standard case. These results could also be used to identify the equivalent fluid properties of such geometry with an inverse method [24].

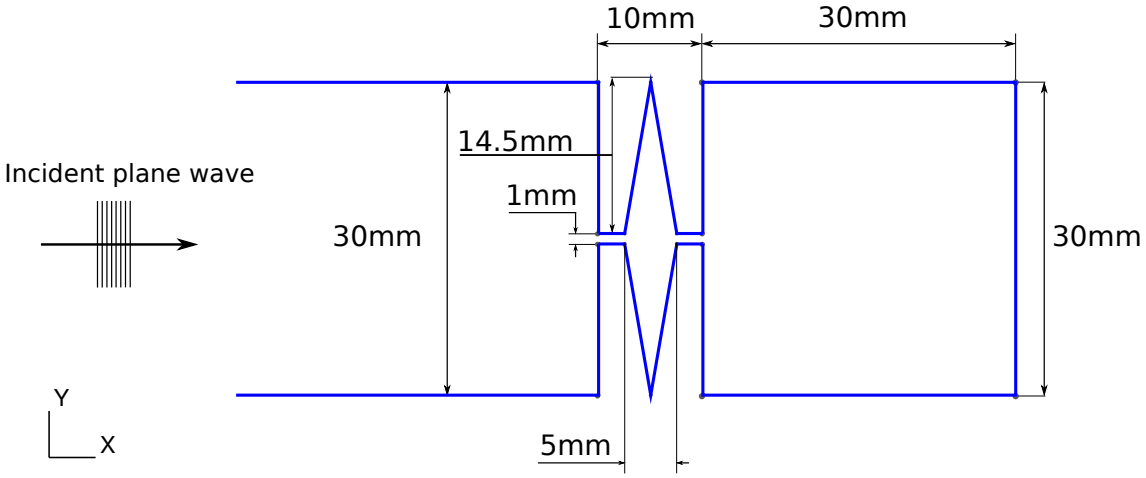

Figure 3: Test case 3

NUMERICAL SIMULATION RESULTS

To evaluate the performance of the two BEM implementations, the sound absorption coefficients in the three test cases are calculated and compared against FLNS-FEM simulations. The FEM calculations are conducted using a system of equations having approximately 2 million degrees of freedom, and a boundary layer mesh with 10 elements in the boundary normal direction. The BEM implementations rely on two different codes, where major parts of the KD-BEM are compiled with C++/MEX and the BLI-BEM is a pure MATLAB implementation. Therefore, it has been decided not to use their computational speed as a measure, but rather their accuracy for different element sizes.

Direct comparison of sound absorption coefficients

In Figure 4 the sound absorption coefficients for the three test cases are shown. The boundary element simulations are using a mesh with a fixed element size of 0.1 mm. In test case 1 (blue data) KD-BEM and BLI-BEM show similar absorption results with a tiny shift in frequency as compared to the FEM reference. It is not uncommon to observe a frequency shift near resonance between FEM and BEM simulations [19]. On the other hand, in test case 2 and test case 3 (the green and red data) some small discrepancies are observed between the reference FEM and the boundary element simulations. It is in particular interesting, that the KD-BEM is slightly underestimating the absorption coefficient near resonance in the two test cases, indicating that higher density meshing is required as compared to the BLI-BEM. It should be noted, that the

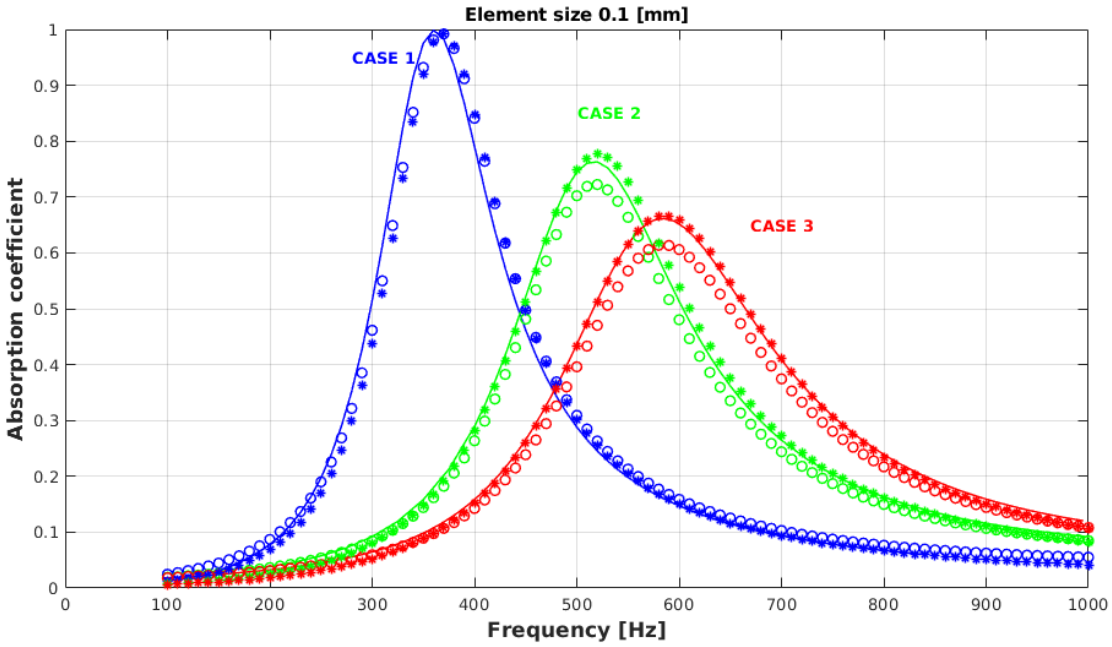

Figure 4: Normal incident sound absorption coefficients for the three test cases. Data are colored blue (test case 1), green (test case 2) and red (test case 3). Solid (-) lines corresponds to FLNS-FEM simulations, circles (o) are KD-BEM simulations, and stars (*) are BLI-BEM simulations. Here, the KD-BEM and BLI-BEM are based on simulations using the same fixed element size of 0.1 mm

two BEM implementations are fundamentally different, relying on two different element types (continuous and discontinuous elements) which might lead to the slightly better results observed when using the BLI-BEM. Moreover, it is also known that discontinuous elements are often superior in BEM computations [25].

The influence of element length (case 2)

To further study the influence of the element size, the absorption coefficients calculated for test case 2 using even coarser meshes are plotted in Figure 5. In the figure, computations corresponding to an element size of 1 mm, 0.5 mm and 0.1 mm are shown. It is observed that for both the KD-BEM and the BLI-BEM a relatively dense mesh is necessary to obtain accurate results.

CONCLUSIONS

The paper has presented three different numerical approaches to incorporate viscous and thermal losses into numerical simulations of acoustic meta-surfaces. Three test cases are proposed, that pose different difficulties if modeled with simpler equivalent fluid models. The focus has mainly been to evaluate the performance of the KD-BEM and the BLI-BEM in terms of their accuracy for a specific element length. Their performance is evaluated through the normal incident absorption coefficient for the three test cases. It is shown that relative dense meshes are required to obtain solutions similar to the reference FLNS-FEM simulations. In general, the BLI-BEM seems to result in slightly less error as compared to the KD-BEM for the same element length. Additionally, the BLI-BEM has

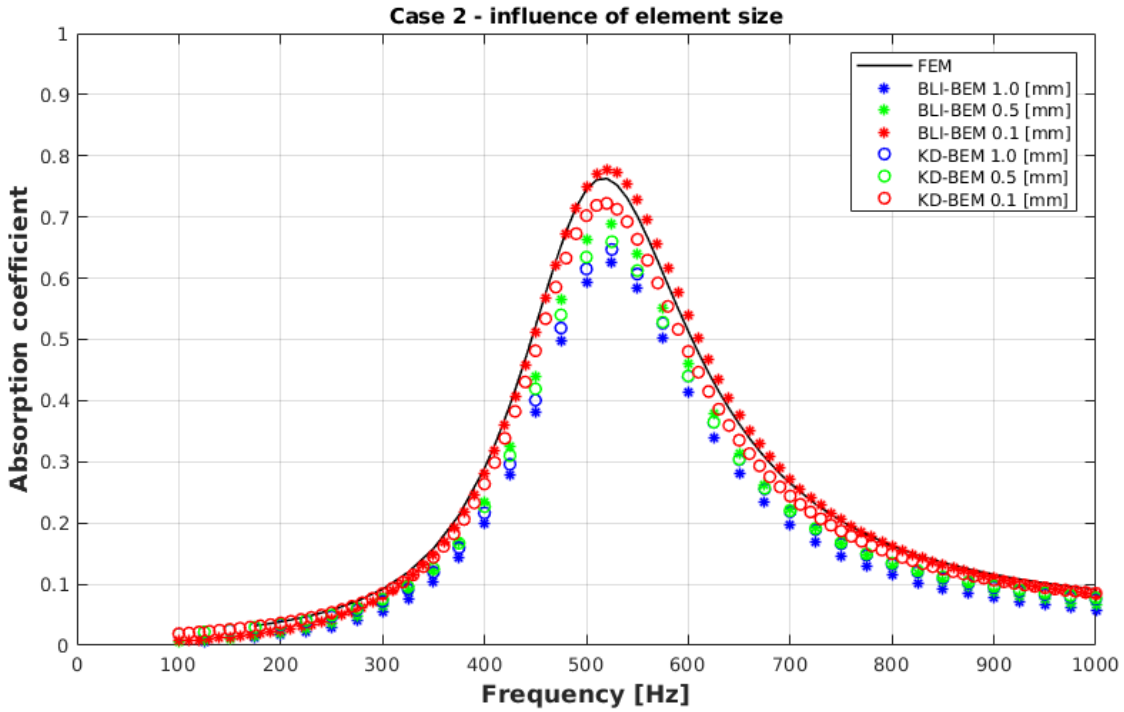

Figure 5: Normal incident absorption coefficients for case 2 using different element sizes. In the figure, the solid black curve is the results for the reference FLNS-FEM model using a very dense mesh, circles (o) correspond to KD-BEM simulations, and stars (*) to BLI-BEM simulations. The boundary element simulations are based on a mesh using there different element sizes, where blue, green and red data corresponds to an element size of 1 mm, 0.5 mm and 0.1 mm, respectively.

similar complexity as the regular isentropic BEM problem making it a good candidate for fast computations and optimization with losses. However, future studies should include test cases that have designs with overlapping boundary layers, and thereby explore the possible limitations of the BLI-BEM method to characterize acoustic meta-surfaces.

ACKNOWLEDGEMENTS

Dissemination of this work was supported by COST (European Cooperation in Science and Technology) through the COST Action CA15125 – DENORMS: “Designs for Noise Reducing Materials and Structures”.

REFERENCES

[1] Y. Li and B. M. Assouar. Acoustic metasurface-based perfect absorber with deep subwavelength thickness. *Appl. Phys. Lett.*, 108:063502, 2016.

[2] H. Ryoo and W. Jeon. Dual-frequency sound-absorbing metasurface based on viscothermal effects with frequency dependence. *Journal of Applied Physics*, 123:115110, 2018.

[3] J. Li, W. Wang, Yangbo Xie, B. Popa, and S. A. Cummer. A sound absorbing metasurface with coupled resonators. *Appl. Phys. Lett.*, 109:091908, 2016.

[4] N. Gao, H. Hou, Y. Zhang, and J. H. Wu. Sound absorption of a new oblique-section acoustic metamaterial with nested resonators. *Modern Physics Letters B*, 32:1850040, 2018.

[5] M. R. Stinson. The propagation of plane sound waves in narrow and wide circular tubes, and generalization to uniform tubes of arbitrary cross-sectional shape. *Journal of the Acoustical Society of America*, 89(2):550–558, 1991.

[6] J. F. Allard and N. Atalla. *Propagation of sound in porous media: modelling sound absorbing materials*. John Wiley & Sons, United Kingdom, 2009.

[7] M. Malinen, M. Lyly, P. Raback, A. Karkkainen, and L. Karkkainen. A finite element method for the modeling of termo-viscous effects in acoustics. In *Proceedings of the 4th European Congress on Computational Methods in Applied and Engineering ECCOMAS, Jyvaskyla, Finland*, 2004.

[8] N. Joly. Finite element modeling of thermoviscous acoustics in closed cavities. In *Proceeding from Acoustics'08, June 29-July 4, Paris (France)*, 2008.

[9] M. J. J. Nijhof, Y. H. Wijant, and A. de Boer. An acoustic finite element including viscothermal effects. In *Proceedings from the 14th International Congress on Sound and vibration, 9-12 july, Cairns (Australia)*, 2007.

[10] L. Cheng, R. D. White, and K. Grosh. Three-dimensional viscous finite element formulation for acoustic fluid-structure interaction. *Computer Methods in Applied Mechanics and Engineering*, 197(49-50):4160–4172, 2008.

[11] W. R. Kampinga, Y. H. Wijnant, and A. de Boer. Performance of Several Viscothermal Acoustic Finite Elements. *Acta Acoustica United with Acustica*, 96(1):115–124, 2010.

[12] V. Cutanda Henríquez and P. M. Juhl. An axisymmetric boundary element formulation of sound wave propagation in fluids including viscous and thermal losses. *Journal of the Acoustical Society of America*, 134(5):3409, 2013.

[13] V Cutanda Henríquez and P. Risby Andersen. A three-dimensional acoustic boundary element method formulation with viscous and thermal losses based on shape function derivatives. *Journal of Computational and Theoretical Acoustics*, 26(3):1859939, 2018.

[14] P. Risby Andersen, V Cutanda Henríquez, N. Aage, and S. Marburg. A two-dimensional acoustic tangential derivative boundary element method including viscous and thermal losses. *Journal of Theoretical and Computational Acoustics*, 26(3):1850036, 2018.

[15] V. Cutanda Henríquez, P.R Andersen, J. S. Jensen, P. M. Juhl, and J. Sánchez-Dehesa. A numerical model of an acoustic metamaterial using the Boundary Element Method including viscous and thermal losses. *Journal of Computational Acoustics*, 25(4):1750006, 2017.

[16] V. Cutanda Henríquez, V.M García-Chocano, and J. Sánchez-Dehesa. Viscothermal losses in double-negative acoustic metamaterial. *Physical Review Applied*, 8(12):014029, 2017.

[17] W. R. Kampinga. *Viscothermal acoustics using finite elements. Analysis tool for engineers*. PhD thesis, University of Twente, Enschede, 2010.

[18] M. Bruneau, Ph. Herzog, J. Kergomard, and J. D. Polack. General formulation of the dispersion equation in bounded visco-thermal fluid, and application to some simple geometries. *Wave Motion 11*, page 441–451, 1989.

[19] P. Risby Andersen, V Cutanda Henríquez, and N. Aage. Shape optimization of micro-acoustic devices including viscous and thermal losses. *Journal of Sound and Vibration*, 447:120–136, 2019.

[20] R. Bossart, N. Joly, and M. Bruneau. Hybrid numerical and analytical solutions for acoustic boundary problems in thermo-viscous fluids. *Journal of Sound and Vibration*, 263(1):69–84, 2002.

[21] K. Schmidt and A Thöns-Zueva. Impedance boundary conditions for acoustic time harmonic wave propagation in viscous gases. 2014.

[22] M.J.J. Nijhof. *Viscothermal wave propagation*. PhD thesis, University of Twente, 2010.

[23] M. Berggren, A. Bernland, and D. Noreland. Acoustic boundary layers as boundary conditions. *Journal of Computational Physics*, 371:633–650, 2018.

[24] Bonglio P. and Pompoli F. Inversion problems for determining physical parameters of porous materials: Overview and comparison between different methods. *JActa Acustica united with Acustica*, 99:341–351, 2013.

[25] S. Marburg and S. Schneider. Influence of Element Types on Numeric error for Acoustic Boundary Elements. *Journal of Computational Acoustics*, 11(3):363–386, 2003.